# Fluid Exchange across a Meandering Jet*

R. M. SAMELSON

*Woods Hole Oceanographic Institution, Woods Hole, Massachusetts*

13 May 1991 and 31 July 1991

ABSTRACT

The motion of fluid parcels in a two-dimensional kinematic model of a meandering jet is investigated using Melnikov's method. The study is motivated by a recent analysis of float trajectories in the Gulf Stream. The results indicate that the efficiency of cross-jet exchange induced by fluctuating meander amplitudes depends strongly on the frequency of the fluctuations. For high frequencies ($\geq$0.04 cpd), exchange between the core of the jet and regions of "trapped" fluid moving with the meander is preferred, while for low frequencies ($\leq$0.04 cpd), exchange between the "trapped" fluid and the slow-moving fluid surrounding the jet is preferred. Propagating waves superimposed on the meandering jet can efficiently cause exchange between regimes when their phase speeds roughly match the basic flow velocities along the regime boundaries. Numerical results suggest that exchange across the center of the jet is less efficient than exchange between adjacent regimes so that the meandering jet will tend to stir fluid along each of its sides but preserve gradients across the jet core.

## 1. Introduction

Fluid exchange across, and mixing within, the Gulf Stream is a poorly understood process that likely plays an important role in determining the distributions of potential vorticity, nutrient concentration, and other fluid properties in the western North Atlantic (e.g., Bower et al. 1985). Clearly, the presence of dynamical properties (such as potential vorticity) that are approximately conserved along parcel trajectories must result in the interdependence of the exchange processes, which are determined by the velocity field, and the velocity field itself, which is determined by the distribution of dynamical properties. Understanding the exchange processes is thus a challenging task, the success of which evidently presumes a simultaneous understanding of the dynamics that govern the evolution of the Gulf Stream. On the other hand, if the velocity field were known, fluid trajectories could be computed without any dynamical considerations. This suggests that kinematic models of fluid exchange, that is, models in which the mixing properties of specified representative velocity fields are studied, may provide a fruitful avenue of approach to this problem.

Such an approach has recently been taken by Bower (1991), who compared RAFOS float observations of the Gulf Stream to fluid trajectories in a velocity field chosen to represent a meandering jet. The velocity field consisted of a jet of uniform width deformed by a steadily propagating sinusoidal meander. In the reference frame moving with the meander, the fluid motion was steady, and for eastward meander propagation, the steady motion in the moving frame was comprised of three regimes: a central jet, exterior retrograde motion, and intermediate closed circulations above meander troughs and below crests. The strength of the intermediate regime was taken as an indicator of exchange, since flow within it alternately resembled flow in the other two regimes. The model predicted that exchange would increase as the difference of the meander phase speed and the maximum zonal velocity in the jet decreased.

In that model, however, no exchange can occur between the three regimes. Fluid parcels in the intermediate regime execute regular oscillations but never escape. Float observations indicate that exchange does occur across (part of) the Gulf Stream; several trajectories that pass through meander crests and troughs and then leave the jet are shown in Fig. 3 of Bower (1991). It is not surprising that the model fails to capture some essential aspects of the observed trajectories since the Gulf Stream is not a uniform jet with a steadily propagating sinusoidal meander. From another point of view, it must be precisely the deviations of the Gulf Stream from the regular pattern of the model that allow exchange. It is then natural to inquire which deviations would cause exchange most efficiently and why.

These questions are pursued here with a model that is a direct descendant of Bower's (1991) meandering jet but includes additional spatiotemporal variability in the velocity field. The model is purely kinematic:

* Woods Hole Oceanographic Institution Contribution Number 7759.

*Corresponding author address:* Dr. Roger Samelson, Woods Hole Oceanographic Institution, Woods Hole, MA 02543.

representative velocity fields are specified without direct consideration of dynamics, and the trajectories of fluid parcels are not constrained by any requirement of potential vorticity conservation. The main tool of the investigation is a method developed by Melnikov (1963) to study the nonlinear stability of dynamical systems and only recently applied to the study of fluid mixing (Knobloch and Weiss, 1987; Rom-Kedar et al. 1990). This method allows efficient estimates of the effect on fluid exchange of spatiotemporal variability that is superimposed on the meandering jet.

The kinematic model is developed and a heuristic discussion of Melnikov's method given in section 2. The main results are in section 3, and section 4 contains a summary.

## 2. The model

### a. The velocity field

The streamfunction for the basic meandering jet is taken to have the form proposed by Bower (1991),

$$\psi(x', y, t) = \psi_0\left[1 - \tanh\left(\frac{y - A\cos k(x' - c_x t)}{\lambda(1 + k^2A^2\sin^2 k(x' - c_x t))^{1/2}}\right)\right], \quad (1)$$

where $x'$ and $y$ are Cartesian coordinates, positive eastward and northward, respectively; $2\psi_0$ is the total eastward transport; $\lambda$ determines the width of the jet; $A$, $k$, and $c_x$ are, respectively, the amplitude, wavenumber, and phase speed of the sinusoidal meander; and the square-root term in the argument of the hyperbolic tangent is inserted to give a uniform jet width through the meander. The two-dimensional velocity field determined by (1) is meant as an idealized representation of flow on an isopycnal surface in a meandering baroclinic jet such as the Gulf Stream. A reference frame moving with the meander may be introduced, with coordinates

$$X = x' - c_x t, \quad Y = y. \quad (2)$$

The corresponding nondimensional streamfunction for motion in the comoving frame is

$$\phi(\xi, \eta) = 1 - \tanh\left[\frac{\eta - B\cos\kappa\xi}{(1 + \kappa^2B^2\sin^2\kappa\xi)^{1/2}}\right] + c\eta, \quad (3)$$

where

$$\phi = \psi_0^{-1}\psi + c\eta, \quad (\xi, \eta) = \lambda^{-1}(X, Y), \quad B = \lambda^{-1}A, \quad \kappa = 2\pi L^{-1} = k\lambda, \quad c = \lambda\psi_0^{-1}c_x \quad (4a)$$

and the nondimensional time and distance are

$$\tau = \psi_0\lambda^{-2}t, \quad x = \lambda^{-1}x'. \quad (4b)$$

With this nondimensionalization, velocities are scaled by the maximum jet velocity in the fixed frame, $\psi_0\lambda^{-1}$. The term in (3) proportional to $\eta$ arises from the motion of the comoving frame. The three parameters $B$ (meander amplitude relative to jet width), $\kappa = 2\pi/L$ (meander wavenumber relative to jet width), and $c$ (meander phase speed relative to maximum jet speed) determine the streamfunction $\phi$ for the basic flow.

Contours of the (nondimensionalized) streamfunction $\psi' = \psi_0^{-1}\psi$ in the fixed frame at $\tau = 0$ are shown in Fig. 1a for $B = 1.2$, $L = 10.$, $c = 0.1$. [This corresponds to the case shown in Fig. 6b of Bower (1991).] Since the streamfunction in the fixed frame is time-dependent, these contours do not correspond to streamlines. The flow in the fixed frame is everywhere eastward, but is modulated by the propagating meander. A profile of Lagrangian mean eastward velocity $U_{LM}$ in the limit $\tau \to \infty$ for parcels initially located along $x = 0$ is shown in Fig. 1b. The jet ($U_{LM} > c = 0.1$) is centered near $\eta = 1.5$, all parcels initially between $\eta \approx -3.5$ and $\eta \approx 0.5$ have $U_{LM} = c$, and parcels north of the jet and south of $\eta \approx -3.5$ have $U_{LM} < c$. Contours of the streamfunction $\phi$ in the comoving frame are shown in Fig. 1c. Since $\phi$ is time independent, these contours correspond to streamlines in the comoving frame and completely describe the flow. As suggested by the profile of Lagrangian mean velocities (Fig. 1b), the flow in the comoving frame is divided into three regimes: a central eastward jet, exterior retrograde relative motion, and closed circulations above meander troughs and below crests. In the closed circulations, the Lagrangian mean fluid velocities are equal to the meander phase speed, and the motion of fluid parcels alternately resembles flow in the jet and exterior regimes. The regimes are separated by two pairs of bounding streamlines, which connect the stagnation points that occur above crests and below troughs. These bounding streamlines are shown in Fig. 1d. (The two northern boundaries are labeled 1 and 2 for reference below.) No fluid crosses these boundaries and there is no exchange between regimes.

In the presence of other variability, the boundaries may break, and exchange between regimes occur. Three different types of variability will be considered here: a time-dependent, spatially uniform meridional velocity superimposed on the basic flow, a time-dependent meander amplitude, and a propagating plane wave superimposed on the basic flow. Time dependence of the meander amplitude may be included in (3) by making $B$ a function of time,

$$B = B_0 + B_1(\tau) = B_0 + \epsilon\cos(\omega\tau + \delta). \quad (5)$$

The meridional flow and the plane wave have nondimensional streamfunctions

$$\phi'(\xi, \eta, \tau) = \xi\cos(\omega\tau + \delta) \quad (6)$$

and

$$\phi'(\xi, \eta, \tau) = \mathrm{p}^{-1}\cos[p(\xi - c_p\tau) + \delta], \quad (7)$$

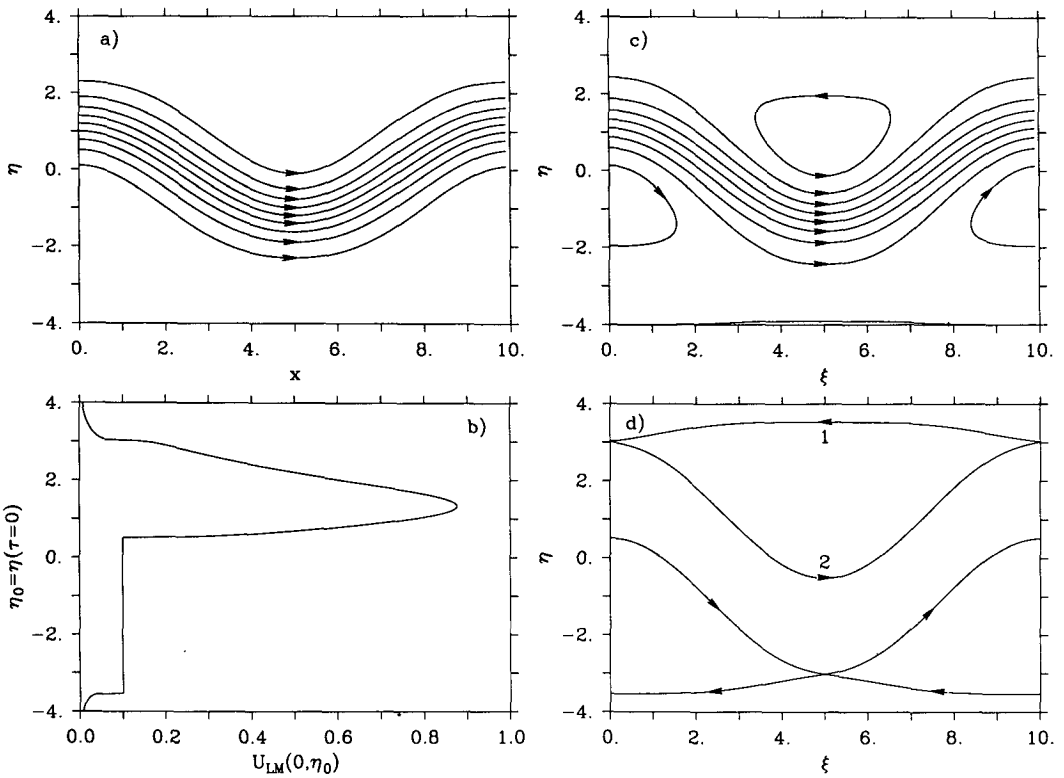


FIG. 1. (a) Contours of the nondimensional streamfunction $\psi' = \psi_0^{-1}\psi$ in the fixed frame at $\tau = 0$ for $B = 1.2$, $L = 10.$, $c = 0.1$. Arrows indicate flow direction. Contour interval: 0.2. (b) Profile of Lagrangian mean eastward velocity for parcels initially located along $x = 0$ in (a). (c) As in (a) but for the streamfunction $\phi$ in the moving frame. (d) Bounding streamlines in the moving frame.

respectively, where $p$ and $c_p$ are the wavenumber and phase speed of the plane wave. The constants $\delta$ are arbitrary.

The corresponding nondimensional velocity field for motion in the comoving frame is

$$u_R = -\Phi_\eta \tag{8a}$$

$$v_R = \Phi_\xi, \tag{8b}$$

where

$$\Phi(\xi, \eta, \tau) = \phi(\xi, \eta; B = B_0 + B_1(\tau)) \tag{9a}$$

for the time-dependent meander amplitude (5) or

$$\Phi(\xi, \eta, \tau) = \phi(\xi, \eta) + \epsilon\phi'(\xi, \tau) \tag{9b}$$

for the uniform meridional flow (6) or propagating plane wave (7). Here, as in (5), $\epsilon$ is a constant that does not need to be small. Parcel trajectories are then determined by integrating the velocity field,

$$\frac{d\xi}{d\tau} = u_R(\xi, \eta, \tau),$$

$$\frac{d\eta}{d\tau} = v_R(\xi, \eta, \tau). \tag{10}$$

Since the velocity field is obtained from a streamfunction, the differential equations (8) and (10) for the parcel trajectories have the form of Hamilton's equations of classical mechanics, with the streamfunction $\Phi$ equivalent to a Hamiltonian function with canonical variables $\xi$ and $\eta$. Aref (1984) noted this coincidence, which has stimulated much recent work on Lagrangian motion in two-dimensional fluids. A similar perspective motivates the present study, although the application of Melnikov's method is not limited to Hamiltonian systems.

Equations (8)–(10) may be solved numerically for any value of $\epsilon$. For small meander amplitude fluctuations ($\epsilon \ll 1$), the streamfunction $\phi(\xi, \eta; B)$ from (9a) may be expanded as

$$\phi(\xi, \eta; B) = \phi(\xi, \eta; B_0) + \epsilon\phi' + O(\epsilon^2),$$

$$\phi' = \frac{\partial\phi}{\partial B}(\xi, \eta; B_0)\cos(\omega\tau + \delta) \tag{11}$$

so that the full motion may be expressed as the basic flow plus a superimposed perturbation as in (9b). Then for all three types of variability, the velocity field (8) may be written

$$u_R = U + \epsilon u, \quad U = -\phi_\eta, \quad u = -\phi'_\eta \quad (12a)$$

$$v_R = V + \epsilon v, \quad V = \phi_\xi, \quad v = \phi'_\xi, \quad (12b)$$

where the $O(\epsilon^2)$ terms from (11) have been neglected for the amplitude fluctuation case. The form (12) is needed for the application of Melnikov's method, which is a perturbation technique formally valid only for $\epsilon \ll 1$.

### b. Melnikov's method

The flow in Fig. 1 is divided into several regimes by two pairs of bounding streamlines ("separatrices"), which connect the stagnation points that occur above meander crests and below troughs (Fig. 1d). In the presence of the variability included in the streamfunction (8), these boundaries may break, and exchange between regimes occur. An analytical technique to detect the breaking of such boundaries ("splitting of separatrices") under small ($\epsilon \ll 1$) time-periodic perturbations was developed by Melnikov (1963), who was interested in the nonlinear stability of dynamical systems. Melnikov's method is the main tool of the present study, but here it is used not on the dynamical flow in phase space, but directly on the velocity field in physical space. The application of Melnikov's method in this general context is briefly reviewed by Ottino (1989). Knobloch and Weiss (1987) and Weiss and Knobloch (1989) have previously used this method to study mixing due to traveling waves. A short description of the method is given here. The full theory contains demanding mathematical technicalities; useful references are Guckenheimer and Holmes (1983) and Lichtenberg and Lieberman (1983). For a recent application of a generalized Melnikov method to the dynamics of a geophysical fluid model, see Allen et al. (1991). Behringer et al. (1991), Pierrehumbert (1991), and Dutkiewicz et al. (personal communication, 1991) have used other (laboratory and numerical) techniques to study the mixing properties of flows similar to (3).

Suppose that the flow varies only slightly from the basic meandering jet, and consider a fluid parcel in the trough of a meander very close to the boundary between the jet and recirculation regimes in the basic flow. The parcel will follow the boundary closely as time progresses, since motion across the streamlines of the basic flow will be driven only by the weak variability. Eventually it will approach the stagnation point above the downstream crest and then either continue downstream (in the jet regime) or return upstream (in the recirculation regime), thereby determining its "regime of destination." Conversely, the parcel's regime of origin may be determined by following it backward in time past the stagnation point above the upstream crest. Since the destination of parcels depends in a continuous way upon their initial positions, instantaneous boundaries will exist that separate parcels according to their regimes of "origin" and "destination." In the time-dependent flow, these boundaries no longer need to correspond to streamlines, and they may even intersect and cross one another. Melnikov's method is a rigorous technique for calculating (to first order in the disturbance amplitude $\epsilon$) the instantaneous local distance between these boundaries. This distance measures the size of the gap through which exchange occurs.

The expression for the Melnikov distance $d$ is

$$d = \epsilon d_M(\tau_0) = \frac{\epsilon M(\tau_0)}{|\mathbf{U}[\mathbf{X}^0(0)]|} \quad (13)$$

where the Melnikov function $M(\tau_0)$ is

$$M(\tau_0) = \int_{-\infty}^{\infty} \{U[\mathbf{X}^0(\tau - \tau_0)]v[\mathbf{X}^0(\tau - \tau_0), \tau] - V[\mathbf{X}^0(\tau - \tau_0)]u[\mathbf{X}^0(\tau - \tau_0), \tau]\} d\tau \quad (14)$$

and $U$, $V$, $u$, and $v$ are defined by (12), and $\mathbf{U} = (U, V)$. The integral (14) is carried out along the bounding streamline $(\xi, \eta) = \mathbf{X}^0(\tau)$ of the basic flow. The distance $d_M(\tau_0)$ is measured normal to the basic flow streamline at the point $(\xi, \eta) = \mathbf{X}^0(0)$ along the streamline. In all the cases considered here, the change of variables $\tau \to \tau' + \tau_0$ in (14) and the use of trigonometric identities leads to an expression of the form

$$M(\tau_0) = M_0 \cos(\omega\tau_0 + \delta'), \quad (15)$$

where $M_0$ and $\delta'$ are determined by the integral over $\tau'$.

Since the basic flow velocity field $(U, V)$ is parallel to the streamline, the Melnikov function $M(\tau_0) = |\mathbf{U}[\mathbf{X}^0(0)]|\, d_M(\tau_0)$ gives the first-order instantaneous volume flux from one regime to the other at $\mathbf{X}^0(0)$. Then the average rate of exchange may be calculated as

$$F = \frac{\omega}{2\pi} \int_0^{2\pi/\omega} \epsilon |M(\tau_0)|\, d\tau_0 = \frac{2}{\pi} \epsilon M_0. \quad (16)$$

The interpretation of this expression has been explored in detail by Rom-Kedar et al. (1990).

The expressions (13) and (14) for the size of the gap $d = \epsilon d_M$ between instantaneous regime boundaries may be derived rigorously by perturbation theory, but the derivation is mathematically demanding, mainly for technical reasons. Since the unit normal $\mathbf{n}$ to a basic flow streamline may be expressed in terms of the basic flow by

$$\mathbf{n} = \frac{(-V, U)}{|\mathbf{U}|}, \quad (17)$$

the integral (14), when normalized to obtain $d_M(\tau_0)$ as in (13), may be heuristically described as the integral of $\mathbf{u} \cdot \mathbf{n}$, an estimate of the distance normal to the bounding streamline that a parcel near that streamline is driven by the time-dependent flow as it traverses a meander. This description is not precise because the denominator $|\mathbf{U}[\mathbf{X}^0(0)]|$ in (13) would have to be

replaced by a term $|\mathbf{U}[\mathbf{X}^0(\tau)]|$ in the denominator of the integrand in (14); from a mathematical point of view, this difference is crucial, since the convergence of the integral (14) often depends on the fact that $|\mathbf{U}[\mathbf{X}^0(\tau)]| \to 0$ as $\tau \to \pm\infty$.

The main topic of interest here is the breakup of the regime boundaries and the resulting exchange of fluid between regimes. The Melnikov method allows an analytical estimate of this effect for small $\epsilon$. However, it is interesting to note that when the Melnikov distance $d_M(\tau_0)$ has simple zeros as a function of $\tau_0$, the regime boundaries intersect and cross one another in a tangle of infinite complexity and flow trajectories become "chaotic" (Guckenheimer and Holmes 1983). In this case, the destinations of parcels near the boundaries will depend sensitively on initial position, with the separation of nearby parcels growing exponentially in time.

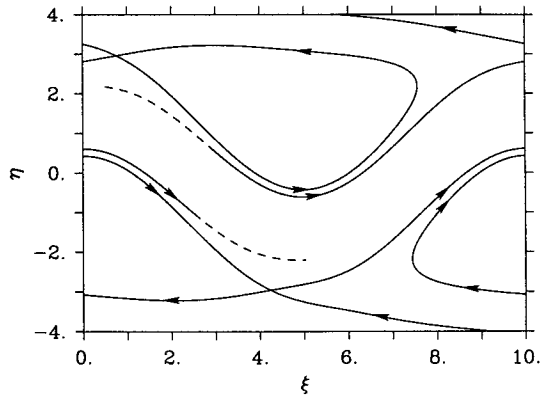


FIG. 2. As in Fig. 1d, but with uniform northward velocity $\epsilon = 0.01$.

## 3. Results

### a. *Spatially uniform meridional flow*

For time-independent spatially uniform northward flow, it is not necessary to use the Melnikov method to determine the exchange across the jet, but the analysis of this simple case is instructive. The total streamfunction for this case is given by (9b) and (6), with $\omega = \delta = 0$. The total northward transport may be obtained by integrating the northward velocity from this streamfunction across one meander wavelength,

$$F_N = \int_0^L \Phi_\xi d_\xi = \epsilon L. \tag{18}$$

The transport may also be obtained from the Melnikov function (14):

$$F_M = \epsilon M(\tau_0) = \epsilon \int_{-\infty}^{\infty} \mathbf{U}[\mathbf{X}^0(\tau - \tau_0)] d\tau = \epsilon L. \tag{19}$$

These two calculations agree, as they must. Since the streamfunction in this case is still time-independent in the comoving frame, contours of the streamfunction are streamlines, and the division of the flow into regimes may be described as in Fig. 1d for the basic flow. The bounding streamlines for this case are shown in Fig. 2 for $\epsilon = 0.01$. Large regions of closed circulation, with $U_{\mathrm{LM}} = c$, still exist, but the boundaries no longer connect upstream and downstream stagnation points, and northward flow through the gaps is allowed. The width of the gap at the midpoint $\xi = 5$ may be estimated from (13) and (19) by $d = \epsilon L/|\mathbf{U}| \approx 0.183$, which compares well with the numerical result 0.182. The trajectories of three parcels initially located along $x = 0$ were followed until $\tau = 150$ (60 days) by integrating (12) for this case. The trajectories in the moving frame are shown in Fig. 3a, along with the bounding trajectories of the basic flow. The southern and northern parcels pass northward through the gaps shown in Fig. 2, the first entering the jet downstream of a trough, and the second leaving the jet upstream of a crest. The third parcel is trapped in a closed regime and executes regular oscillations. The trajectories in the fixed frame are shown in Fig. 3b, and their (nondimensional) zonal coordinates $x = \xi + c\tau$ are shown versus time $\tau$ in Fig. 3c, in which the transitions into and out of the jet are indicated by changes in slope.

When the uniform meridional flow is time dependent [$\omega \neq 0$ in (6)], the integrals similar to (18) and (19) yield different quantities: (18) still gives the instantaneous net northward flow

$$F_N(\tau) = \epsilon L \cos(\omega\tau + \delta), \tag{20}$$

but the result of (14), the Melnikov function $M(\tau_0)$,

$$M(\tau_0) = \int_{-\infty}^{\infty} \mathbf{U}[\mathbf{X}^0(\tau - \tau_0)] \cos(\omega\tau + \delta) d\tau \tag{21}$$

measures the instantaneous flow through the gap between regimes at the point $(\xi, \eta) = \mathbf{X}^0(0)$ of the bounding trajectory and depends on the frequency $\omega$ and phase $\delta$ of the oscillatory meridional flow. For $\omega \neq 0$, (20) shows that the average northward transport is zero, but this now does not imply that the average rate of exchange between regimes vanishes, only that northward and southward transports balance in the mean. The integral (21) takes the form (15), and the resulting $M_0$ is plotted in Fig. 4 for the two bounding trajectories north of the jet. Results for the flow south of the jet are identical by symmetry. By (16), the average rate of exchange is proportional to $M_0$. The values of $M_0$ for the boundary between the recirculation regime and the jet are larger (except at $\omega = 0$) than for the boundary between the recirculation and the retrograde motion regimes, indicating that exchange across the former boundary is more efficiently generated by the fluctuating meridional flow. This is due in part to differences in the size of the gap $d$, and in part to the difference in basic flow speed along the bounding trajectories. For both boundaries, $M_0$ approaches a

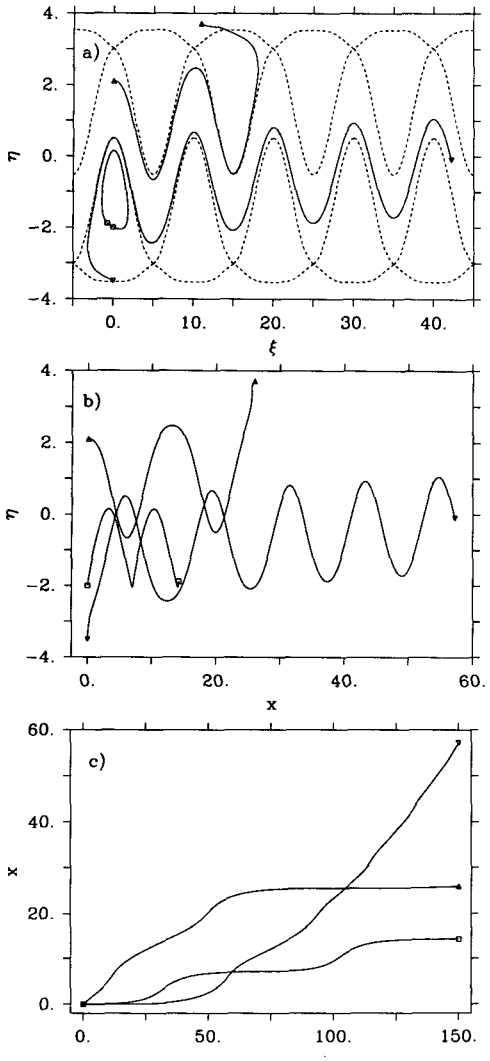


FIG. 3. (a) Trajectories of parcels in the moving frame, with uniform northward velocity $\epsilon = 0.01$. Dashed lines: bounding trajectories as in Fig. 1d. (b) As in (a) but in the fixed frame. (c) Zonal position in fixed frame versus time for trajectories in (b).

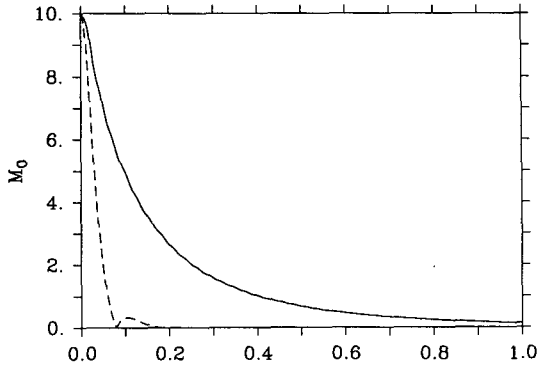


FIG. 4. Amplitude $M_0$ of the Melnikov function versus frequency for oscillatory meridional flow. Solid line: results for boundary 2, between jet core and northern recirculation cell. Dashed line: results for boundary 1, between northern recirculation cell and northern retrograde regime.

maximum at $\omega = 0$, where it takes the value obtained directly in (17) and (18) for the constant meridional flow.

Several trajectories for the flow with $\omega = 0.2$, $\epsilon = 0.03$ are shown in Fig. 5. These may be compared with trajectories shown in Fig. 3 for the case of constant meridional flow. Exchange between the jet and the recir-

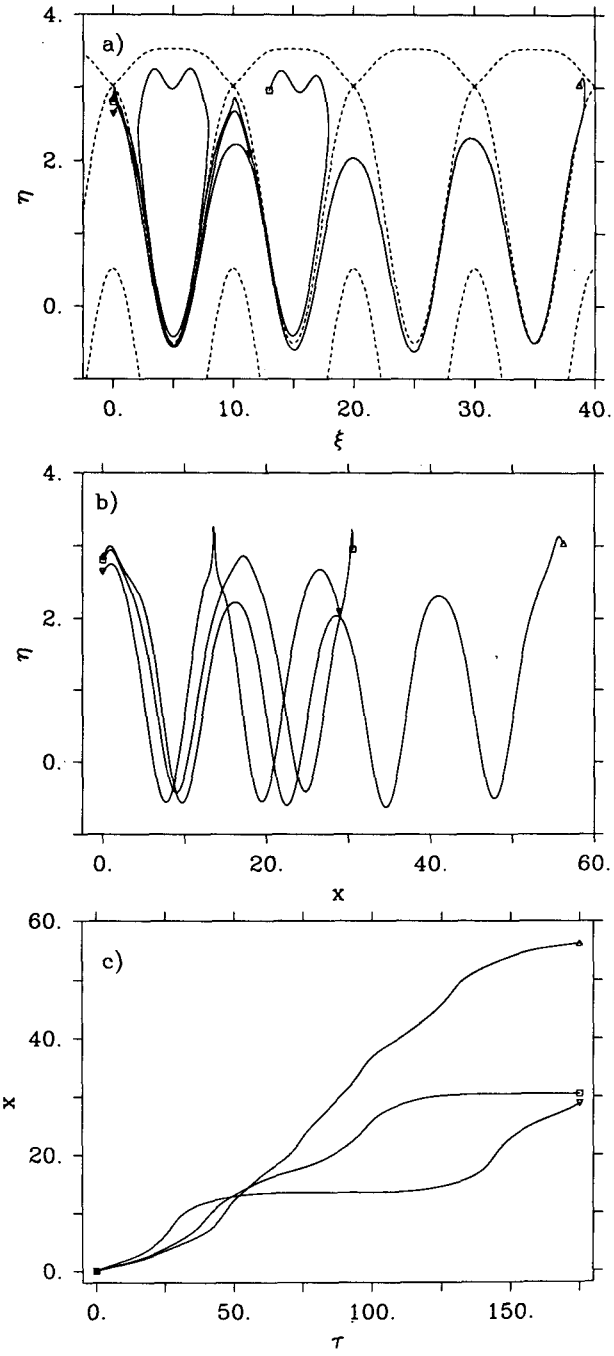


FIG. 5. As in Fig. 3, but for oscillatory meridional velocity, $\omega = 0.2$, $\epsilon = 0.03$.

culation cells occurs in both directions in Fig. 5. The trajectory marked by the inverted triangle starts in the jet, traces one loop around the first recirculation, and then rejoins the jet. Note that the trajectory with the southernmost starting point in Fig. 5 is the first to exit the jet toward the north, while the northernmost remains in the jet the longest, exactly opposite to what might be naively anticipated. Figure 5c may be compared with Fig. 3 of Weiss and Knobloch (1989), who refer to exchange between regimes as "trapping and untrapping" of parcels.

For the time-dependent meridional flow, the streamfunction in the moving frame is time-dependent, and contours of the streamfunction no longer correspond to streamlines, so a simple picture similar to Fig. 3a cannot be drawn. The instantaneous regime boundaries, which are the analogs of the boundaries shown in Fig. 3a, now intersect each other. However, the flow can be visualized in a "Poincaré section," a snapshot of the motion at a fixed phase of the periodically fluctuating flow. (This is a well-known technique in Hamiltonian dynamics.) The geometry of the exchange is sketched in Fig. 6a, in which the instantaneous regime boundaries at some time $\tau_0 = \tilde{\tau}_0$ (phase $\tilde{\theta} = \omega\tilde{\tau}_0 + \delta$) are shown schematically in the moving frame. Arrows indicate the flow in the jet and the recirculation cell, and the intersecting lines represent (parts of) the regime boundaries. One boundary splits the flow according to a parcel's "regime of origin," and one according to its "regime of destination," with one end of each boundary lying in the (upstream or downstream, respectively) dotted circle near the stagnation points of the basic flow. The other end of each boundary is enmeshed in an infinitely complex "homoclinic tangle" (Guckenheimer and Holmes 1983) of which only the first few bends are shown in the figure. At time $\tau_0 = \tilde{\tau}_0 + 2\pi/\omega$, the picture is identical, since the velocity field is periodic in time, but the fluid parcels have moved: those in region A to region B, and those in region a to region b. The parcels moving from A to B leave the jet and join the recirculation, while those moving from **a** to **b** do the opposite. The correspondence between this motion and the Melnikov distance $d$ is illustrated in Fig. 6b, where $d$ is shown for $\mathbf{X}^0(0)$ slightly upstream of $\xi = 5$ in region a, along with parts of the regime boundaries from Fig. 6a. The flow from left to right through the gap measured by $d$ corresponds to fluid leaving the recirculation, in agreement with the characterization of the exchange associated with parcels moving from region a to b in Fig. 6a. Rom-Kedar et al. (1990) describe in detail a similar geometry of exchange for flow due to an unsteady vortex pair.

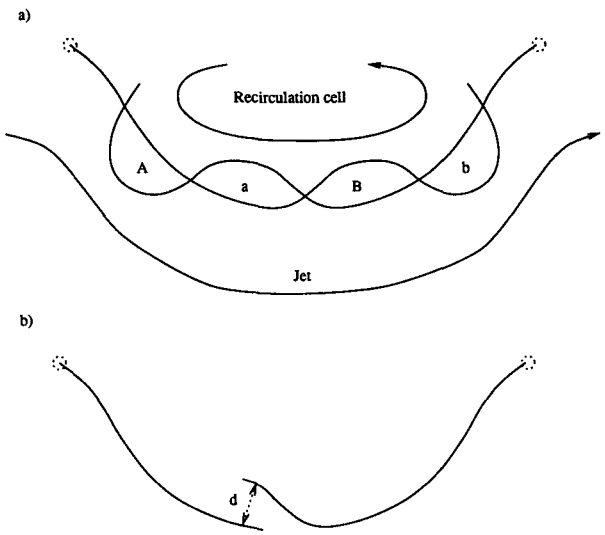


FIG. 6. Sketch of instantaneous regime boundaries for oscillatory flow. (a) Fluid in regions A and a move to regions B and b, respectively, after one oscillation. (b) The Melnikov distance $d$.

The remaining calculations focus on the Melnikov function, which provides a compact estimate of the amount of exchange between regimes. The trajectories of exchanged parcels are similar in character to those shown in Fig. 5 for the oscillating meridional flow. The weak superimposed variability slowly drives parcels across the basic flow streamlines, but on short time scales the trajectories tend to follow those streamlines. The character of trajectories in the presence of strong variability, for which the Melnikov method formally is inapplicable, is briefly considered in section 3d.

### *b. Fluctuating meander amplitude*

Fluctuations in the amplitude of meanders constitute a major part of observed Gulf Stream variability. It is thus natural to investigate the effect on fluid exchange of fluctuations (5) in the meander amplitude $B$ in the kinematic model. Results may be conveniently obtained from the Melnikov method for small fluctuations, ($\epsilon \ll 1$), for which the expansion (11) allows the use of the Melnikov method.

The results (again for the two bounding trajectories north of the jet) are shown in Fig. 7. In contrast to the results for oscillatory meridional flow, the exchange vanishes at $\omega = 0$, as it must, since by (5) this corresponds to choosing a different constant value of $B$. Maximal exchange between the jet and recirculation occurs for $\omega \approx 0.35$ (0.14 cpd) and falls off more rapidly for lower frequencies than higher. The most striking feature of Fig. 7 is the relative difference in the strength of the exchange across the two boundaries. Both the maximum exchange and the frequency range over which significant exchange occurs are an order of magnitude larger for the boundary between the jet and the recirculation than for that between the recirculation and the retrograde motion. As for the oscillating meridional flow, this difference is due in part to the lower basic flow velocities along the latter boundary. At low

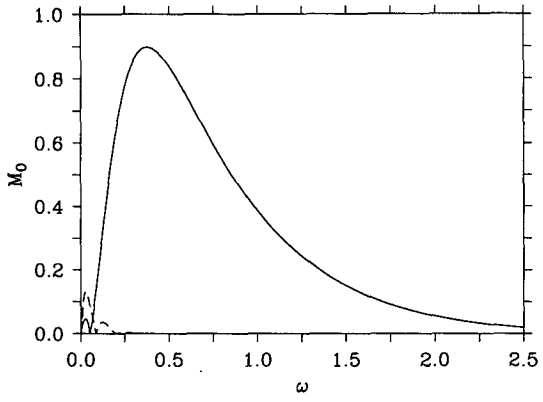


FIG. 7. As in Fig. 4, but for fluctuating meander amplitude.

frequency ($\omega \approx 0.04$, 0.016 cpd), however, the exchange across the latter boundary is more than twice that across the former.

The size and character of the regimes of the basic flow described by (3) depend on the difference $1 - c$ of the jet's peak zonal velocity and the meander phase speed (Bower 1991), so it might be expected that the exchange induced between these regimes by fluctuations in the meander amplitude also depends in an essential way on this difference. Figure 8 shows the results for $c = 0.05$ and $c = 0.2$. (The nondimensional values $c = 0.05$, 0.1, and 0.2 correspond to Bower's (1991) cases of peak jet velocity at 200, 100, and 50 cm $s^{-1}$, respectively. For $c = 0.05$, a secondary recirculation regime occurs near the stagnation points, but this regime is small and the associated exchange is negligible and not shown.) The results are qualitatively similar to those for $c = 0.1$, but peak exchange and the frequency at which peak exchange occurs both increase with increasing $c$ (decreasing $1 - c$).

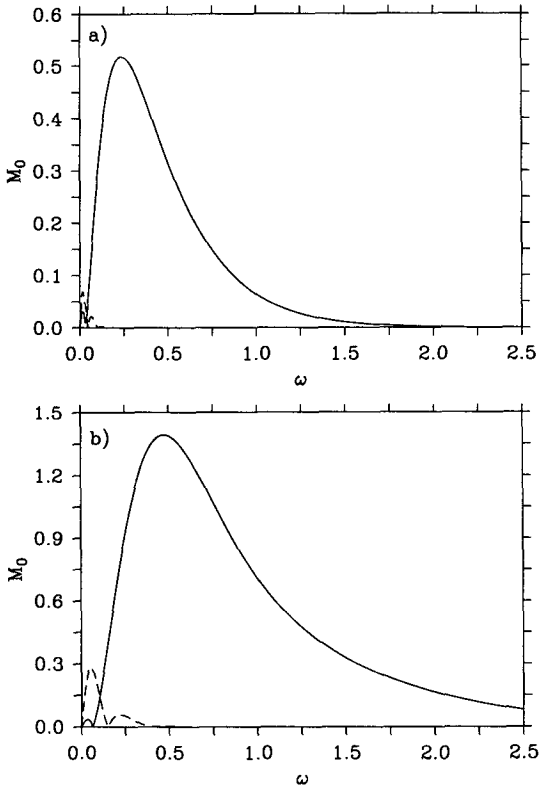


FIG. 8. As in Fig. 7, but for $c$ = (a) 0.05, (b) 0.2.

### c. *Propagating plane waves*

In the model of Bower (1991), the meridional displacement of parcels in a meandering jet was shown to depend on the difference $1 - c$ of the maximum jet velocity and the meander phase speed $c$. This result has a simple physical interpretation: if this difference is small, a parcel initially located in a section of the

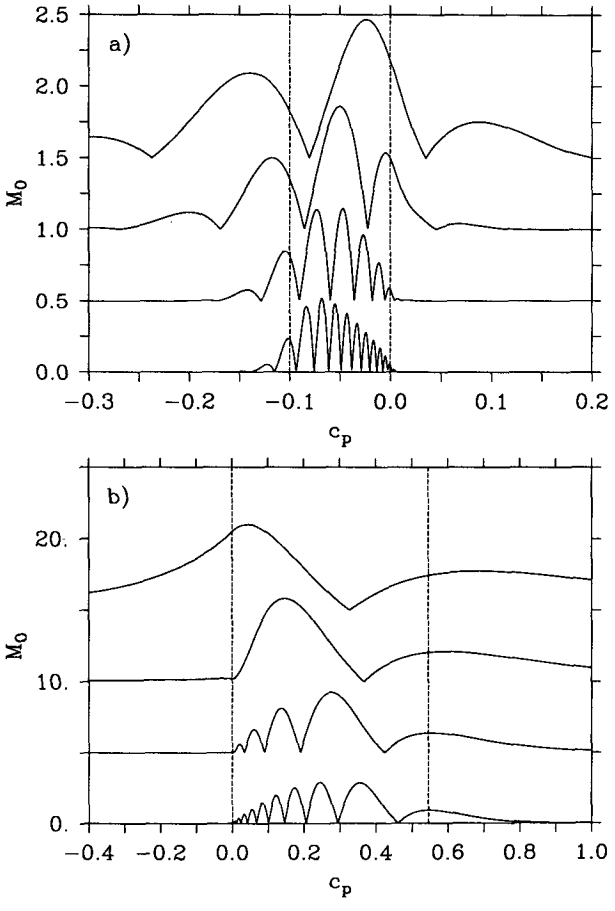


FIG. 9. Amplitude $M_0$ of the Melnikov function versus plane wave phase speed $c_p$ for plane wave with wavelengths $L_p$ = 1, 2, 5, 10, offset successively by 0.5 in (a) and 5 in (b). Results for boundaries between (a) northern recirculation cell and northern retrograde regime and (b) jet core and northern recirculation cell. Dashed lines: maximum and minimum basic flow zonal velocities along corresponding regime boundaries.

meander with (say) a northward component of velocity will remain in that section of the meander for a relatively long time and will be advected relatively far northward by the persistent northward flow. A qualitatively similar, but quantitatively less exact, result holds for exchange induced between flow regimes by zonally propagating plane waves in the present model.

The streamfunction for the zonally propagating plane waves is given by (7). Here the wavelength of the plane wave is restricted so that an integer number of waves fits in the basic flow meander wavelength $L$. Figure 9 shows results of the Melnikov calculation (for the basic case $c = 0.1$) versus the phase speed $c_p$ of the plane wave for four different plane wave wavelengths, $L_p = 1$, 2, 5, and 10. The maximum and minimum zonal velocities along the corresponding bounding streamlines of the basic flow are shown as vertical dashed lines. As the wavelength $L_p$ decreases, the exchange is confined ever more strictly to the range of phase speeds between these maximum and minimum velocities. Conversely, for the longest wavelength, $L_p = 10$, relatively strong exchange is found over a broad band of phase speeds. The oscillations of $M_0$ as $c_p$ varies are related to detailed resonance conditions within the

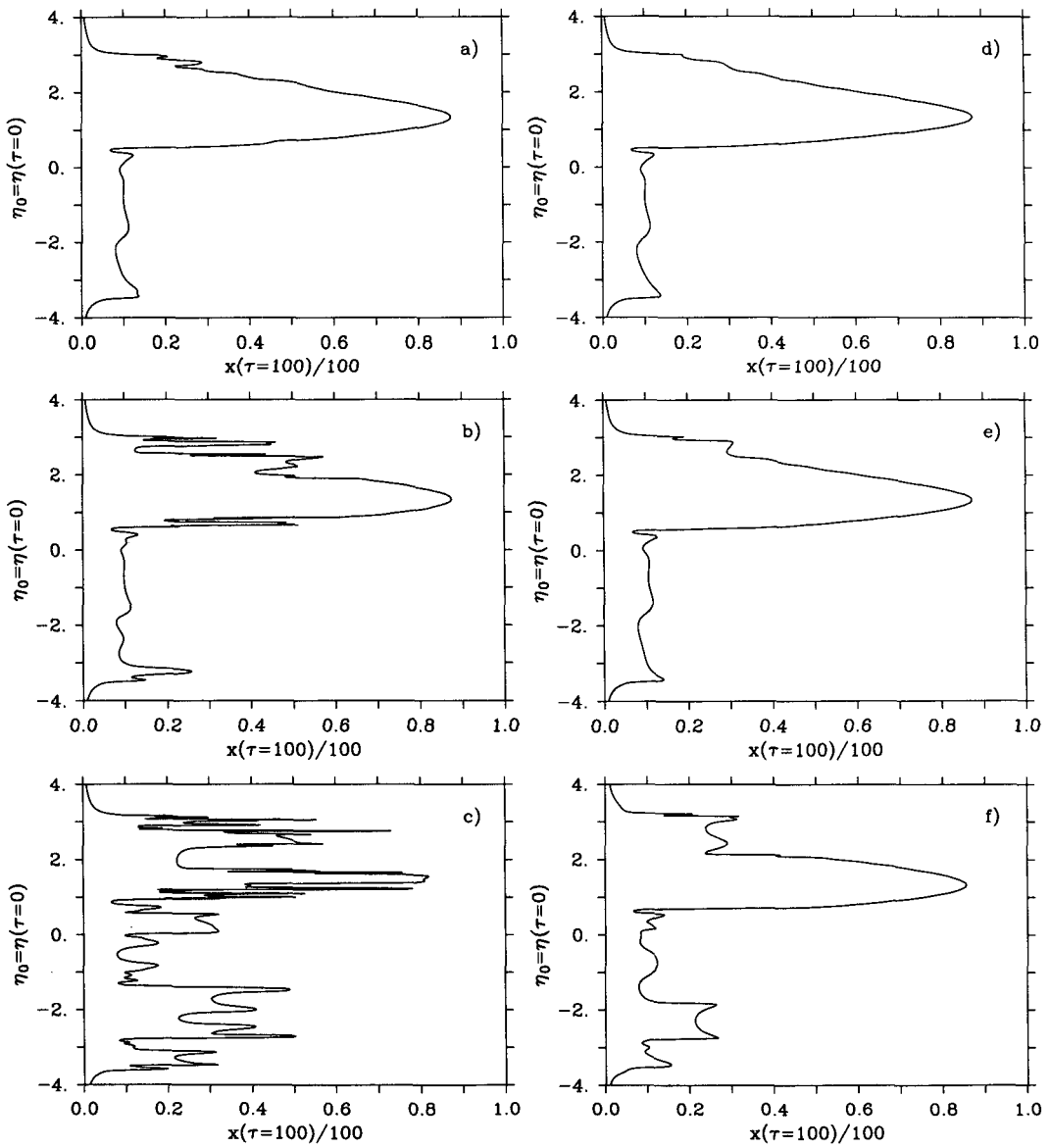


FIG. 10. Lagrangian mean eastward velocity $x(\tau = 100)/100$ for parcels initially located along $x = 0$ for various values of the amplitude $\epsilon$ and frequency $\omega$ of meander fluctuation. (a, b, c) $\omega = 0.25$, (d, e, f) $\omega = 0.1$; (a, d) $\epsilon = 0.01$, (b, e) $\epsilon = 0.1$, (c, f) $\epsilon = 0.5$.

periodic flow, and their physical meaning is less robust than the correspondence between the plane wave phase speed for enhanced exchange and the velocity along the bounding trajectory of the basic flow.

### d. *Finite amplitude variability*

The deviations of Gulf Stream meanders from a regular periodic pattern with constant phase propagation are clearly large relative to the amplitude of the meanders themselves (even disregarding such catastrophes as ring formation). While the Melnikov method is a perturbation method that applies formally only for small amplitude deviations from the basic flow, the results can prove to be a useful guide to finite amplitude behavior in the present kinematic model. In this section, the predictions of the Melnikov analysis for fluctuating meander amplitude (section 3b) are briefly compared to numerical results on exchange induced by large fluctuations.

The profile of Lagrangian mean zonal velocity $U_{LM}$ in the limit $\tau \to \infty$ for parcels initially located along $x = 0$ is shown in Fig. 1b for the basic flow ($c = 0.1$). A set of similar but finite-time, Lagrangian mean zonal velocity profiles is shown in Fig. 10 for various values of the amplitude $\epsilon$ and frequency $\omega$ of the meander fluctuation (5). These profiles have been obtained numerically from the positions at $\tau = 100$ (40 days) of 500 points initially located along $x = 0$. The amount of exchange between regimes may be estimated by comparing these profiles to the exact $U_{LM}$ profile in the absence of fluctuations (Fig. 10b). (Some deviations from the exact profile are to be expected even without exchange, since asymptotic values will not have been reached by $\tau = 100$.) The relative strength of the exchange at the different frequencies is indicated by the Melnikov results (Fig. 6) even at finite amplitude.

These calculations also indicate that exchange across the jet core is much weaker than exchange between regimes. Thus, the fluctuations in meander amplitude evidently stir the fluid along each side of the jet more efficiently than across the jet core. This is qualitatively consistent with observed property distributions in the upper Gulf Stream, which indicate a sharp front in the jet and weak gradients elsewhere (e.g., Bower et al. 1985). A dramatic laboratory demonstration of this effect is given by Behringer et al. (1991).

## 4. Summary

The exchange of fluid parcels between regimes of a kinematic model of a meandering jet has been investigated with the method of Melnikov. The results indicate that the efficiency of exchange induced by fluctuating meander amplitudes depends strongly on the frequency of the fluctuations. For high frequencies ($\omega \geqslant 0.04$ cpd for typical Gulf Stream scales), exchange between the jet and the regions of trapped fluid moving with the meander is preferred, while for low frequencies ($\omega \leqslant 0.04$ cpd), exchange between the trapped regime and the slow-moving fluid surrounding the jet is preferred. Propagating plane waves can efficiently cause exchange between regimes when their phase speeds match the basic flow velocities along the regime boundary. Numerical results suggest that exchange across the center of the jet is more difficult to achieve than exchange between adjacent regimes, so that the meandering jet will tend to stir fluid along each of its sides but preserve gradients across the jet core. In this sense, the Gulf Stream may act as both a "blender" and a "barrier" at its upper levels, thereby maintaining a sharp front between the water masses that it divides. Ring formation, which is not treated (even kinematically) in the present model, may provide more efficient cross-frontal exchange. The present kinematic results must be treated with caution, and more realistic dynamical models must be devised and analyzed. Nonetheless, this simple model should prove useful to future studies that include direct consideration of dynamics.

*Acknowledgments.* I am grateful to A. Bower for discussions and comments. N. Hogg and J. Pedlosky also made useful suggestions. S. Lozier and J. Weiss gave useful comments on the manuscript. This research was supported by the Office of Naval Research under Grant N00014-91-J-1570 and the National Science Foundation under Grant OCE-9101461.

## REFERENCES

Allen, J. S., R. M. Samelson, and P. A. Newberger, 1991: Chaos in a model of quasigeostrophic flow over topography: An application of Melnikov's method. *J. Fluid Mech.*, **226,** 511–547.

Aref, H., 1984: Stirring by chaotic advection. *J. Fluid Mech.*, **143,** 1–21.

Behringer, R., S. Meyers, and H. Swinney, 1991: Chaos and mixing in a geostrophic flow. *Phys. Fluids, A,* **3,** 1243–1249.

Bower, A. S., 1991: A simple kinematic mechanism for mixing fluid parcels across a meandering jet. *J. Phys. Oceanogr.*, **21,** 173–180.

——, H. T. Rossby, and J. L. Lillibridge, 1985: The Gulf Stream—barrier or blender? *J. Phys. Oceanogr.*, **15,** 24–32.

Guckenheimer, J., and P. Holmes, 1983: *Nonlinear Oscillations, Dynamical Systems, and Bifurcations of Vector Fields.* Springer, 453 pp.

Knobloch, E., and J. B. Weiss, 1987: Chaotic advection by modulated travelling waves. *Phys. Rev. A,* **36,** 1522–1524.

Lichtenberg, A. J., and M. A. Lieberman, 1983: *Regular and Stochastic Motion.* Springer, 499 pp.

Melnikov, V. K., 1963: On the stability of the center for time-periodic perturbations. *Trans. Moscow Math. Soc.*, **12,** 1–57.

Ottino, J. M., 1989: *The Kinematics of Mixing: Stretching, Chaos, and Transport.* Cambridge, 364 pp.

Pierrehumbert, R. T., 1991: Large-scale horizontal mixing in planetary atmospheres. *Phys. Fluids, A,* **3,** 1250–1260.

Rom-Kedar, V., A. Leonard, and S. Wiggins, 1990: An analytical study of transport, mixing, and chaos in an unsteady vortical flow. *J. Fluid Mech.*, **214,** 347–394.

Weiss, J. B., and E. Knobloch, 1989: Mass transport and mixing by modulated traveling waves. *Phys. Rev. A,* **40,** 2579–2589.